

# **Loss of function of the nuclear envelope protein LEMD2 causes DNA damage-dependent cardiomyopathy**

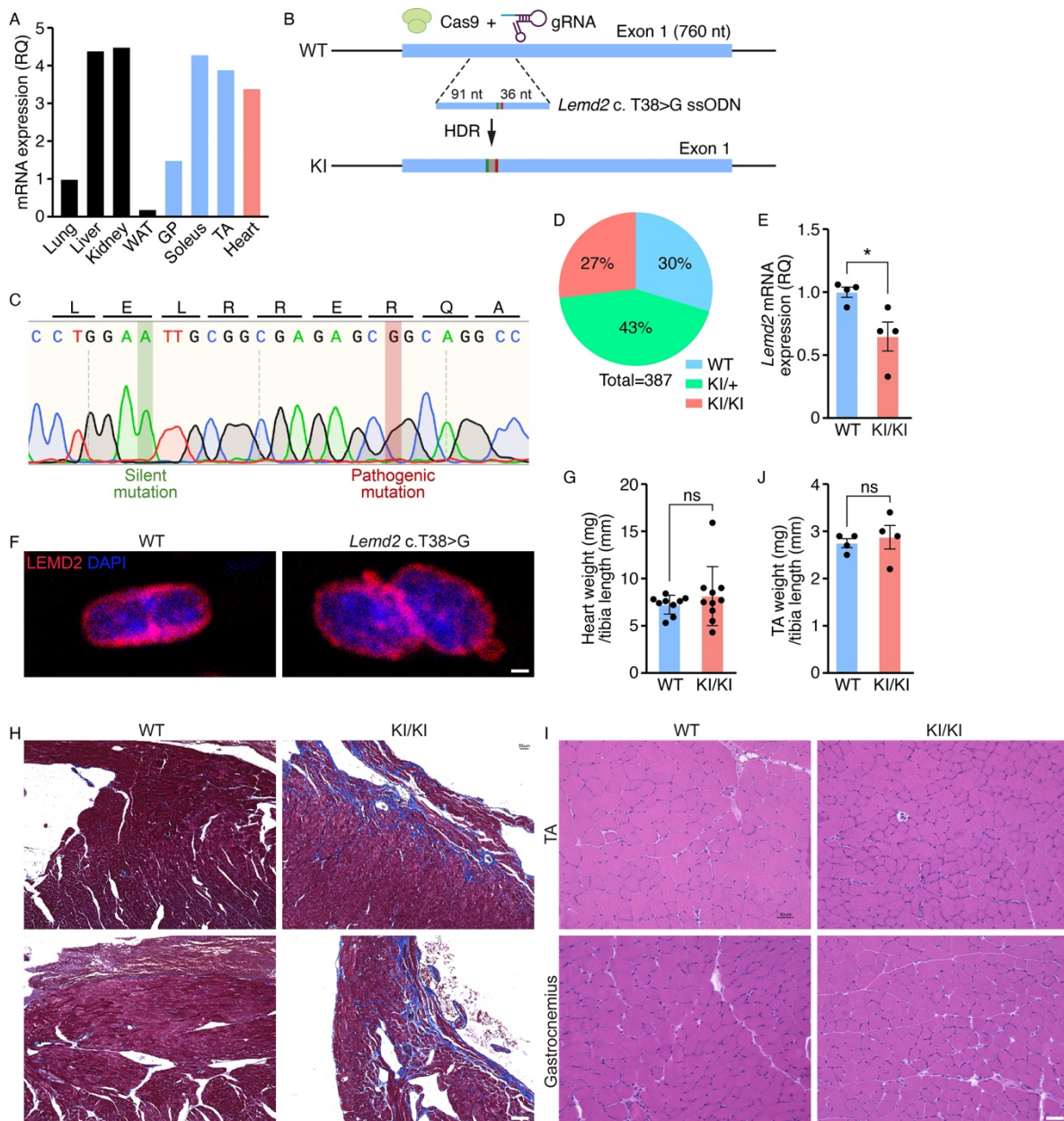
Xurde M. Caravia<sup>1,2</sup>, Andres Ramirez-Martinez<sup>1,2</sup>, Peiheng Gan<sup>1,2</sup>, Feng Wang<sup>3</sup>, John R. McAnally<sup>1,2</sup>, Lin Xu<sup>3</sup>, Rhonda Bassel-Duby<sup>1,2</sup>, Ning Liu<sup>1,2</sup> & Eric N. Olson<sup>1,2,\*</sup>

<sup>1</sup>Department of Molecular Biology, Hamon Center for Regenerative Science and Medicine, University of Texas Southwestern Medical Center, Dallas, TX, USA. <sup>2</sup>Senator Paul D. Wellstone Muscular Dystrophy Specialized Research Center, University of Texas Southwestern Medical Center, Dallas, TX, USA. <sup>3</sup>Quantitative Biomedical Research Center, Department of Population & Data Sciences and Department of Pediatrics, University of Texas Southwestern Medical Center, Dallas, TX, USA.

\*Corresponding author: Eric N. Olson, Ph.D.; Mailing address: UT Southwestern Medical Center. Department of Molecular Biology. 6000 Harry Hines Blvd. Dallas, TX 75390-9148; Phone: +1 214-648-1187; Email: [eric.olson@utsouthwestern.edu](mailto:eric.olson@utsouthwestern.edu)

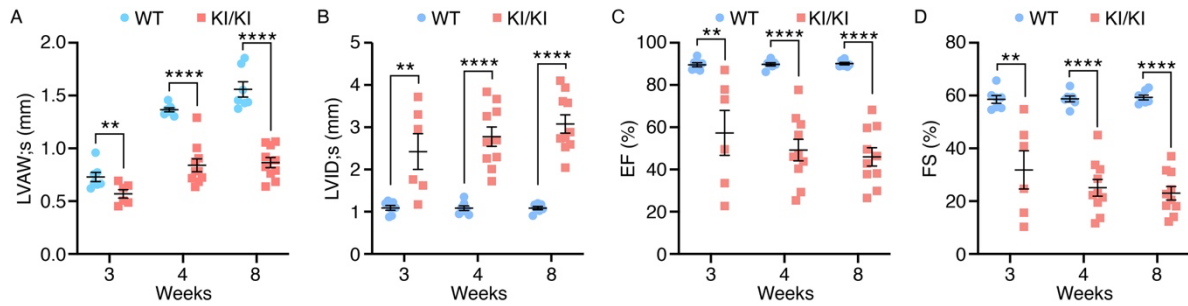
**Supplemental information**

## Supplemental figures



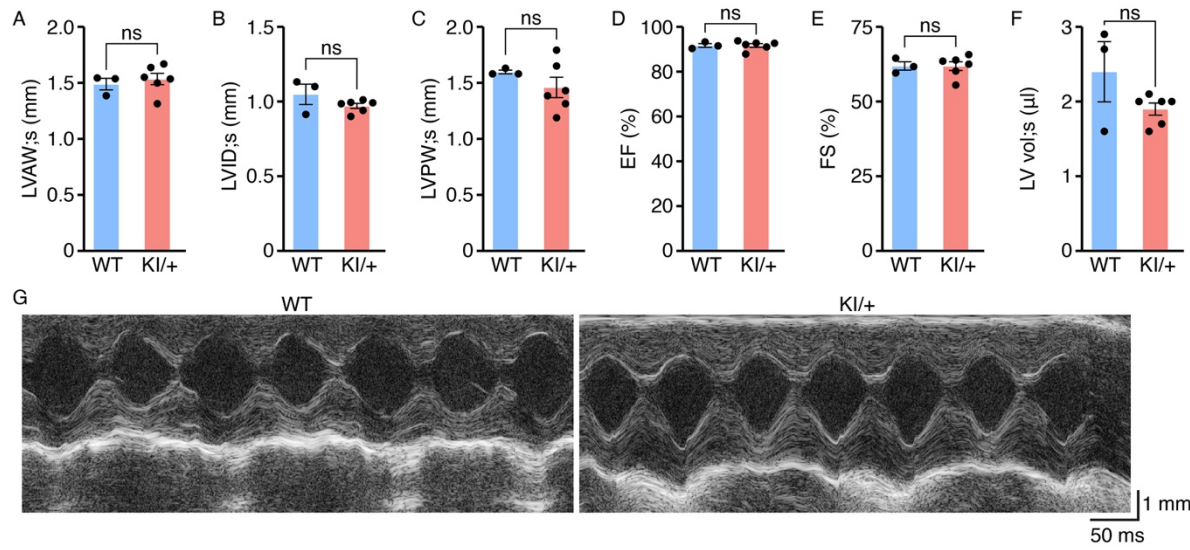
**Supplemental Figure 1: Generation and characterization of the KI/KI mouse model.** **A)** *Lemd2* mRNA expression in mouse tissues normalized to lung (GP, gastrocnemius-plantaris; TA, tibialis anterior; WAT, white adipose tissue). **B)** Schematic of the CRISPR/Cas9 strategy to generate the KI/KI mice. **C)** Sanger sequencing of a KI/KI mouse. **D)** Genotype frequency distribution seven days after birth (P7) of WT, KI/+

and KI/KI mice from heterozygous breeding (387 mice,  $p =$  non-significant; Chi-square test). **E)** *Lemd2* mRNA expression relative to *Gapdh* in hearts from 2-month-old WT ( $n = 4$ ) and KI/KI ( $n = 4$ ) mice ( $*p < 0.05$ ; two-tailed unpaired t test). **F)** Immunofluorescence showing the localization of LEMD2 WT and LEMD2 c.T38>G after their retroviral overexpression in C2C12 myotubes (scale bar: 10  $\mu\text{m}$ ). **G)** Heart weight / tibia length ratio in WT and KI/KI mice (ns (non-significant)  $p > 0.05$ ; two-tailed unpaired t test). **H)** Masson Trichrome staining of hearts from WT and KI/KI mice (scale bar: 50  $\mu\text{m}$ ). **I)** H&E staining of tibialis anterior (TA) and gastrocnemius muscle groups from WT and KI/KI mice (scale bar: 50  $\mu\text{m}$ ). **J)** Tibialis anterior (TA) weight / tibia length ratio in WT and KI/KI mice (ns (non-significant)  $p > 0.05$ ; two-tailed unpaired t test).

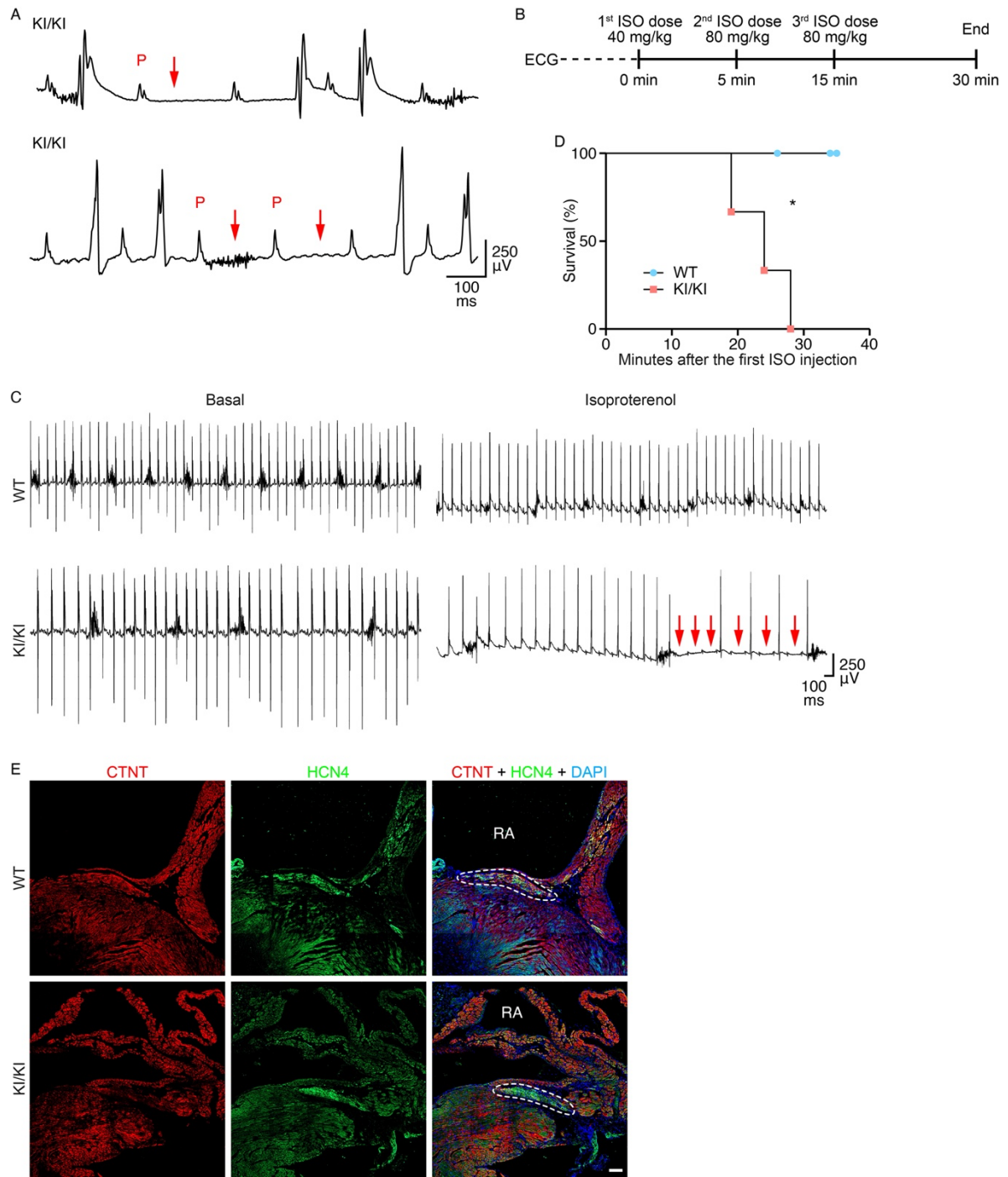


**Supplemental Figure 2: KI/KI mice develop DCM.** Echocardiographic analysis of structural and functional parameters in systolic hearts from WT and KI/KI mice: **A)** Systolic left ventricular anterior wall (LVAW;s) thickness (3w \*\*p<0.01, 4w \*\*\*\*p<0.0001, 8w \*\*\*\*p<0.0001, two-tailed unpaired student t test). **B)** Systolic left ventricular internal diameter (LVID;s) (3w \*\*p= 0.01, 4w \*\*\*\*p<0.0001, 8w \*\*\*\*p<0.0001, two-tailed unpaired student t test), **C)** Ejection fraction (EF) (3w \*\*p<0.01, 4w \*\*\*\*p<0.0001, 8w \*\*\*\*p<0.0001, two-tailed unpaired student t test) and **D)** Fractional shortening (FS) (3w \*\*p<0.01, 4w \*\*\*\*p<0.0001, 8w \*\*\*\*p<0.0001, 7 WT and 6 KI/KI mice for the 3w comparison and 7 WT and 10 KI/KI mice for the 4w and 8w comparisons; two-tailed unpaired student t test).



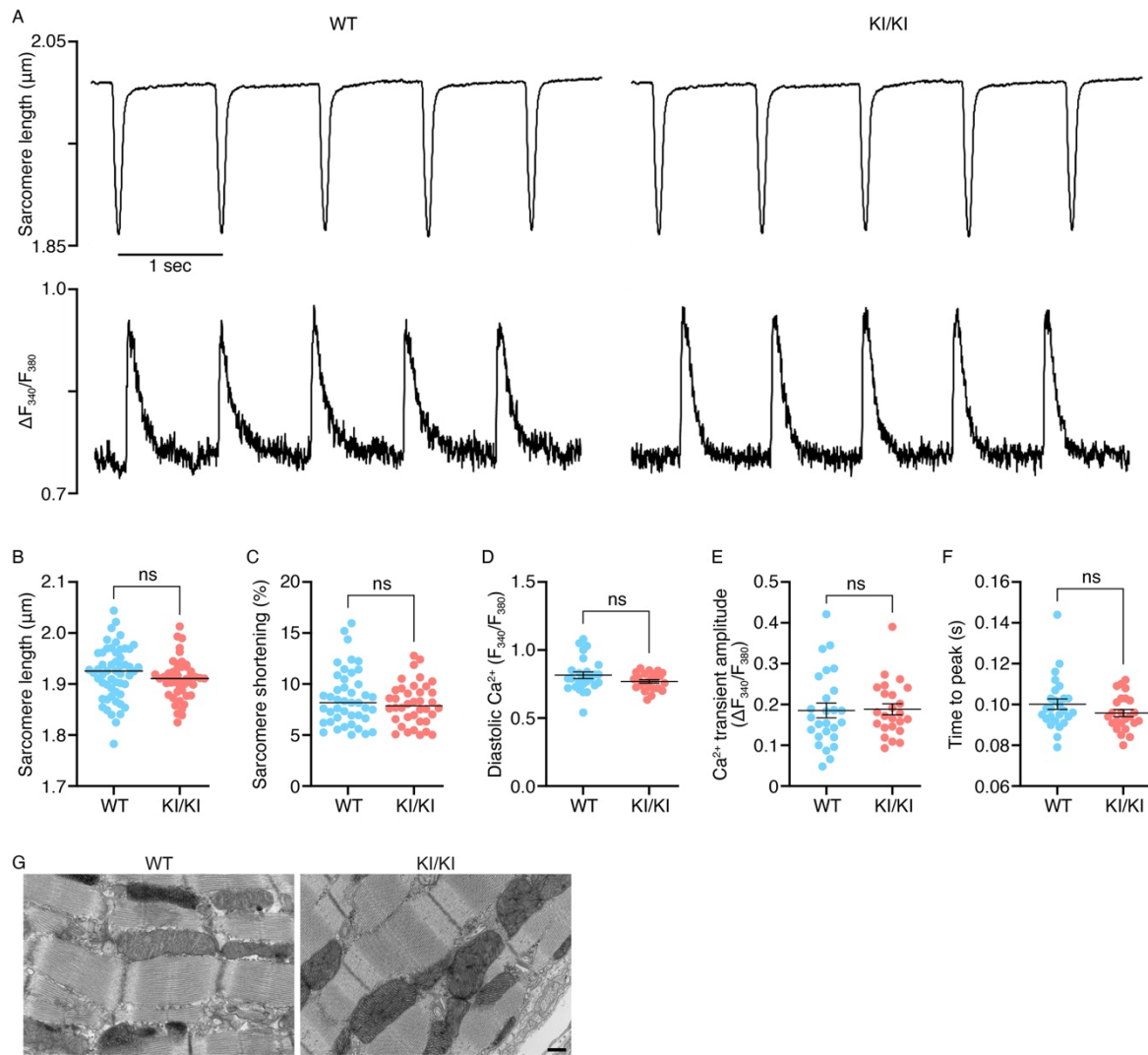


**Supplemental Figure 3: Mice heterozygous for the *Lem2* c.T38>G (KI/+) mutation have a preserved cardiac function.** Echocardiographic analysis of structural and functional parameters in systolic hearts from 2-month-old WT (n=3) and KI/+ mice: **A)** Systolic left ventricular anterior wall (LVAW;s) thickness, **B)** Systolic left ventricular internal diameter (LVID;s), **C)** Systolic left ventricular posterior wall (LVPW;s) thickness, **D)** Ejection fraction (EF), **E)** Fractional shortening (FS) and **F)** Left ventricle volume (n=6). **G)** Representative transthoracic M-mode echocardiographic tracings of 2-month-old WT and KI/+ mice. (ns (non-significant)  $p > 0.05$ ; two-tailed unpaired t test for all the comparisons).

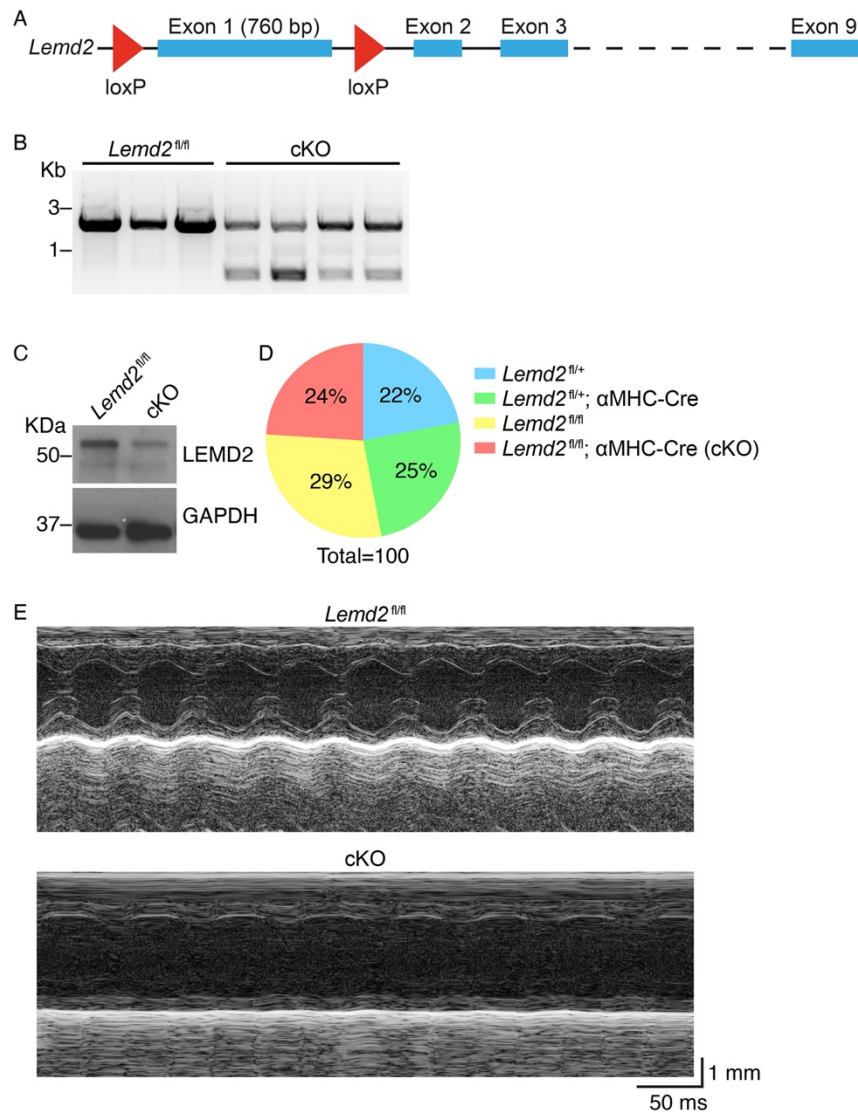


**Supplemental Figure 4: KI/KI mice show cardiac electrical abnormalities. A)** ECG of two 2-month-old KI/KI mice showing the type II AV block (arrows indicate the absence of the QRS complex). **B)** Schematic of the isoproterenol (ISO) administration protocol. **C)** Representative ECG from mice at 4-5 months old before (basal) and after ISO administration (arrows indicate the absence of the QRS complex). **D)** Survival curve of

WT (n=3) and KI/KI (n=3) mice after the first ISO administration (Log-rank (Mantel-Cox) test; \*p<0.05). **E)** Immunostaining of cardiac sections from WT and KI/KI mice against the CM marker cardiac troponin T (cTnT) and the cardiac conduction system-specific marker HCN4. (White lines mark the AV node; RA: right atrium; scale bar: 100  $\mu$ m).

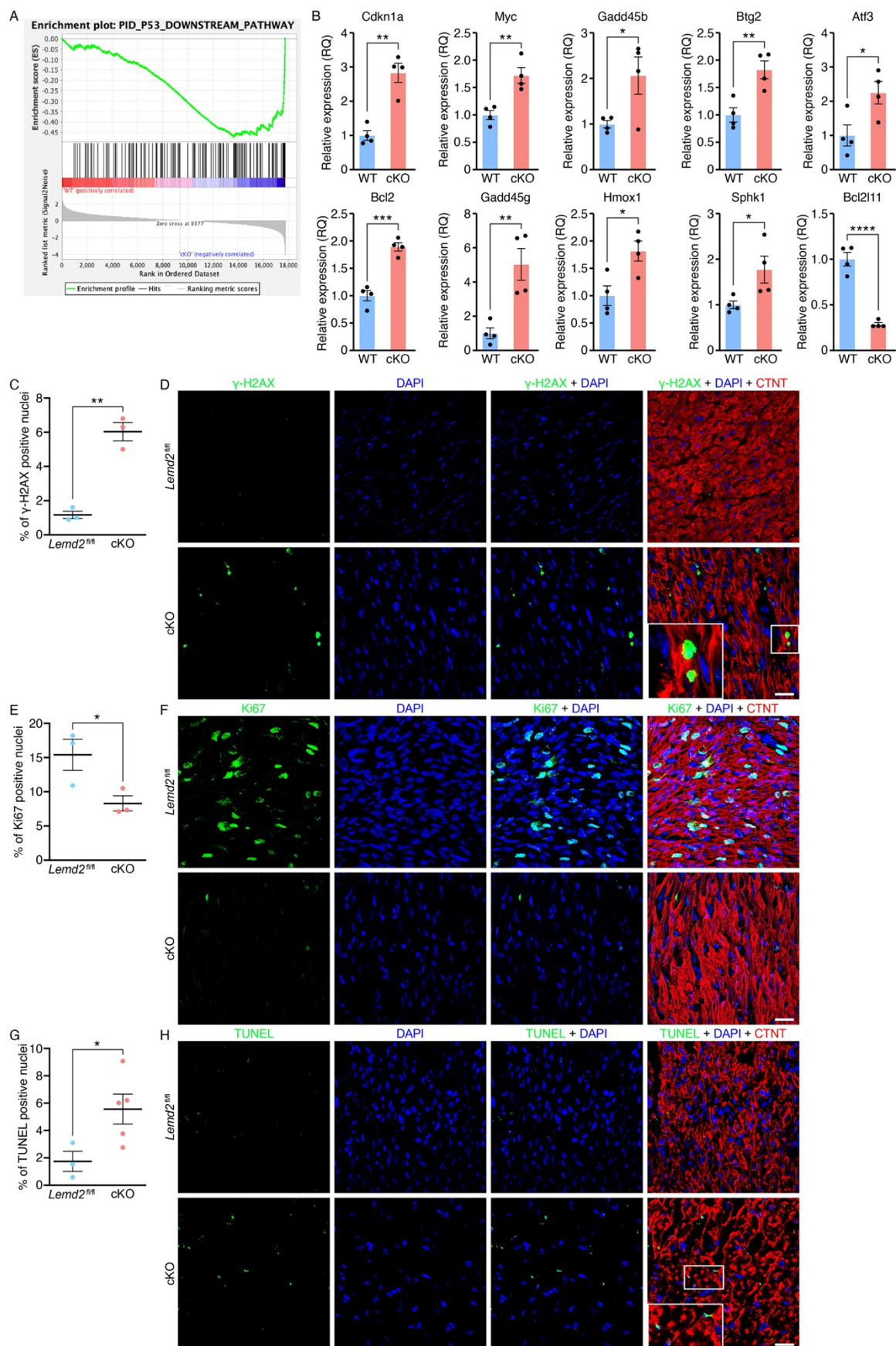


**Supplemental Figure 5: Structure, sarcomere contractility and calcium dynamics in KI/KI isolated CMs.** **A)** Representative sarcomere contraction (top) and calcium transients (bottom) of WT and KI/KI CMs. **B)** Sarcomere length in CMs from WT (n=4) and KI/KI (n=3) mice. **C)** Percentage of sarcomere fractional shortening in CMs from WT (n=4) and KI/KI (n=3) mice. **D)** Ratio of diastolic calcium levels ( $F_{340}/F_{380}$ ) measured using the Fura-2 dye in CMs from WT (n=4) and KI/KI (n=3) mice. **E)** Calcium transient amplitude (from basal level to peak) measured using the Fura-2 dye in CMs from WT (n=4) and KI/KI (n=3) mice. **F)** Time to calcium peak measured using the Fura-2 dye in CMs from WT (n=4) and KI/KI (n=3) mice. **G)** Representative transmission EM pictures of the sarcomere structure of 3-month-old WT and KI/KI hearts (scale bar: 2  $\mu\text{m}$ ). (ns (non-significant)  $p > 0.05$ ; two-tailed unpaired t test for all the comparisons).



**Supplemental Figure 6: Generation and characterization of cKO mice. A)** Scheme showing the *Lemd2*-floxed allele. **B)** PCR showing the excision of the *Lemd2*-floxed allele (first exon) in cardiac tissue after the expression of the recombinase Cre under control of the αMHC promoter (floxed band=1.5 Kb; KO band=80bp). **C)** Western blot analysis showing the expression of both LEMD2 cardiac isoforms in heart protein lysates from *Lemd2*<sup>fl/fl</sup> and cKO mice. **D)** Genotype frequency distribution one day after birth (P1) of mice from *Lemd2*<sup>fl/+</sup> αMHC-Cre x *Lemd2*<sup>fl/fl</sup> breeding (100 mice, p= non-significant; Chi-square test). **E)** Transthoracic M-mode echocardiographic tracings of P7 *Lemd2*<sup>fl/fl</sup> and cKO mice.





**Supplemental Figure 7. Activation of p53 signaling pathway, DNA damage and cellular apoptosis in cKO mice.** **A)** GSEA plot showing the enrichment of genes related p53 downstream pathway in cKO mice. Note that the enrichment score (green line) deviates from 0 in the right part of the plot, indicating that those genes are enriched in the cKO mice (3 mice per genotype). **B)** mRNA expression, normalized to 18S, of genes related to p53 signaling and DDR in WT and cKO hearts (4 mice per genotype; Cdkn1a \*\*p<0.01, Myc \*\*p<0.01, Gadd45b \*p<0.05, Btg2 \*\*p<0.01, Atf3 \*p<0.05, Bcl2 \*\*\*p<0.001, Gadd45g \*\*p<0.01, Hmox1 \*p<0.05, Sphk1 \*p<0.05 and Bcl2l1 \*\*\*\*p<0.0001; two-tailed unpaired t test). **C)** Quantification of the percentage of nuclei positive for  $\gamma$ -H2AX staining in *Lemd2<sup>fl/fl</sup>* and cKO hearts (3-4 mice per genotype, more than 100 nuclei per mouse, \*\*p<0.01 two-tailed unpaired t test). **D)** Representative pictures of  $\gamma$ -H2AX staining in cardiac sections from P5 *Lemd2<sup>fl/fl</sup>* and cKO mice (scale bar: 20  $\mu$ m). **E)** Quantification of the percentage of nuclei positive for Ki67 staining in *Lemd2<sup>fl/fl</sup>* and cKO hearts (3 mice per genotype, more than 500 nuclei per mouse, \*p=0.048 two-tailed unpaired t test). **F)** Representative pictures of Ki67 staining in cardiac sections from P5 *Lemd2<sup>fl/fl</sup>* and cKO mice (scale bar: 20  $\mu$ m). **G)** Quantification of the nuclei positive for TUNEL staining in *Lemd2<sup>fl/fl</sup>* and cKO mice (3-4 mice per genotype, more than 100 nuclei per mouse, \*\*p=0.0493 two-tailed unpaired t test). **H)** Representative pictures of TUNEL staining in cardiac sections from P5 WT and cKO mice (scale bar: 20  $\mu$ m).



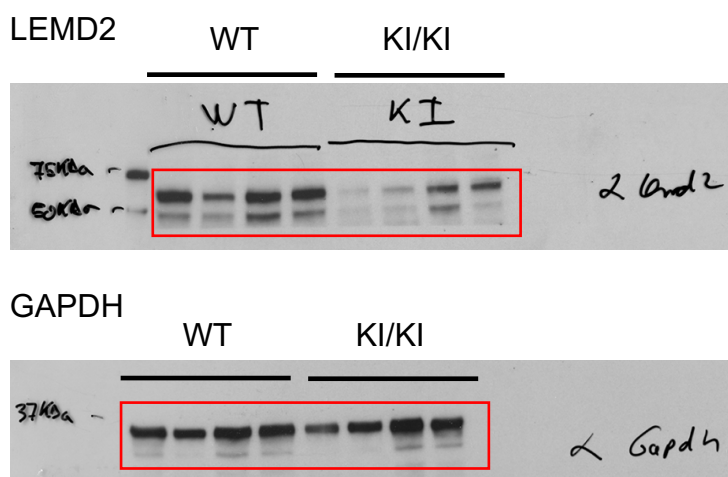
**Supplemental Table 1. Sequences of the primers used for RT-qPCR gene expression analysis.**

<b>Primer ID</b>	<b>Sequence (5' -&gt; 3')</b>
Atf3_Fw	AAGACTGGAGCAAAATGATG
Atf3_Rv	GTCAGGTTAGCAAAATCCTC
Bcl2_Fw	ATGACTGAGTACCTGAACC
Bcl2_Rv	ATATAGTTCCACAAAGGCATC
Bcl2l11_Fw	ACGAGTTCAACGAAACTTAC
Bcl2l11_Rv	TAGATCCTGTCAATGCCTTC
Btg2_Fw	CTGACCGATCATTACAAACAC
Btg2_Rv	AGACACTTCATAGGGATCAAC
Gadd45g_Fw	CTGCAGATCCATTTCACG
Gadd45g_Rv	TTAGGATTGCAAATGAGGATG
Hmox1_Fw	CATGAAGAACTTTCAGAAGGG
Hmox1_Rv	TAGATATGGTACAAGGAAGCC
Sdc1_Fw	CTTCTGTCATCAAAGAGGTTG
Sdc1_Rv	CAAAGGTGAAGTCTTGTTCTC
Sphk1_Fw	GGTACTCTCATCTCGACTTC
Sphk1_Rv	GCCAGATTTTTAGCTTCCAG
Cdkn1a_Fw	ACCTGATGATACCCAACACTAC
Cdkn1a_Rv	CTGTGGCACCTTTTATTCTG
Myc_Fw	TTTTGTCTATTTGGGGACAG
Myc_Rv	CATAGTTCCTGTTGGTGAAG
Gadd45b_Fw	TGCAATCTTCTTTTACCCC
Gadd45b_Rv	CAAGAGCAAAGTACAAGTCC
Lemd2_Fw	GACTGTGAGAGAAMACAGATG
Lemd2_Rv	CACATTAGCTATGTACTCCTG
Gapdh_Fw	AGGTCGGTGTGAACGGATTTG
Gapdh_Rv	TGTAGACCATGTAGTTGAGGTCA
18S_Fw	CCATCCAATCGGTAGTAGCG
18S_Rv	GTAACCCGTTGAACCCATT

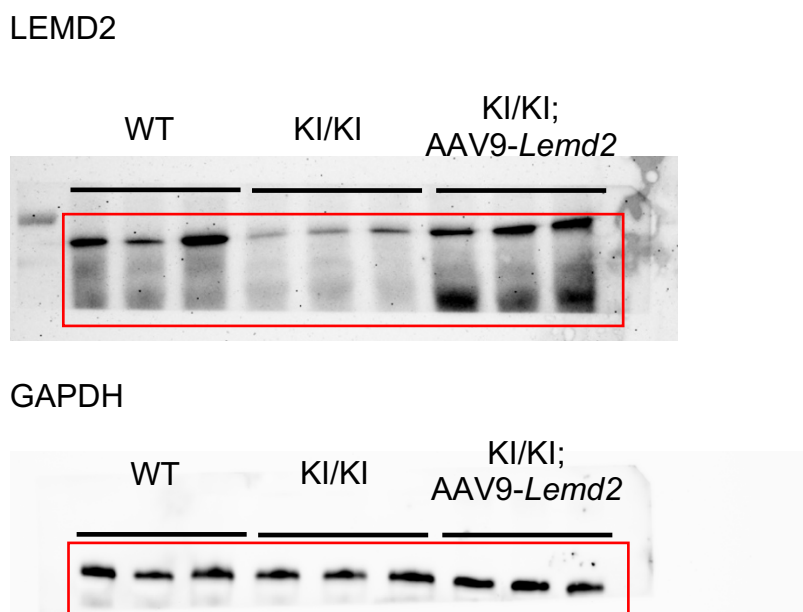
**Unedited versions of all gel and blot images included in the manuscript entitled  
“Loss of function of the nuclear envelope protein LEMD2 causes DNA damage-  
dependent cardiomyopathy”**

Lanes highlighted in red are included in the figures.

- Full unedited protein blot for Figure 1C:

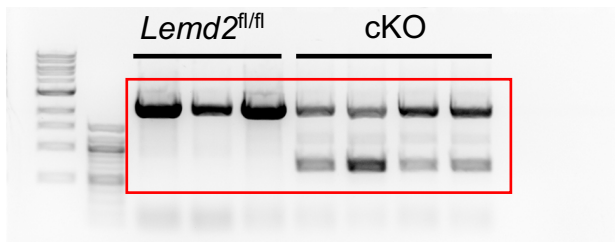


- Full unedited protein blot for Figure 7L:



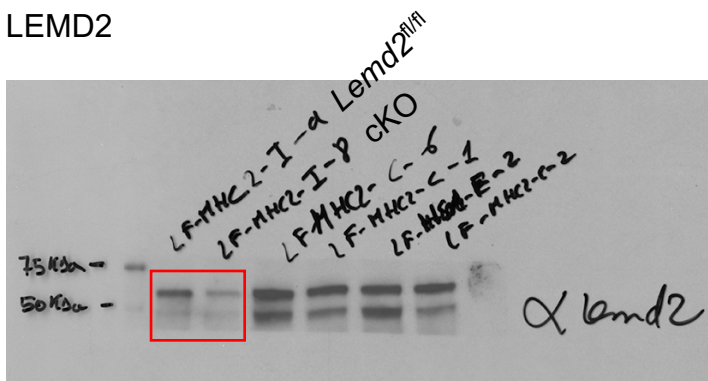
- Full unedited DNA gel for Supplemental Figure 6B:

Lemd2 (DNA excision)



- Full unedited protein blot for Supplemental Figure 6C:

LEMD2



GAPDH

